hsa_circ_0017842 acts as a competing endogenous RNA to enhance the malignancy of gastric cancer

*Xigang Wen[1,A,D,F], *Wenling Han[2,B–D,F], Chao Liu[1,E,F]

[1] Department of Gastrointestinal Surgery, Third People's Hospital of Hubei Province, Wuhan, China
[2] Department of Hospital Infection, Third People's Hospital of Hubei Province, Wuhan, China

A – research concept and design; B – collection and/or assembly of data; C – data analysis and interpretation;
D – writing the article; E – critical revision of the article; F – final approval of the article

Advances in Clinical and Experimental Medicine, ISSN 1899–5276 (print), ISSN 2451–2680 (online) *Adv Clin Exp Med*. 2023;32(7):803–812

Address for correspondence
Chao Liu
E-mail: ChaoLiu53@163.com

Funding sources
None declared

Conflict of interest
None declared

* Xigang Wen and Wenling Han contributed equally to this work.

Received on June 21, 2022
Reviewed on June 29, 2022
Accepted on December 23, 2022

Published online on March 30, 2023

Abstract

Background. Circular RNAs (circRNAs) have been shown to act as competing endogenous RNAs (ceRNAs) participating in the progression of gastric cancer (GC).

Objectives. Our study aimed to investigate whether hsa_circ_0017842 can affect the malignancy of GC in a ceRNA manner.

Materials and methods. Gene expression microarrays from GEO DataSets database, quantitative real-time polymerase chain reaction (qPCR) and western blotting were used to identify the expression levels of hsa_circ_0017842, miR-1294, and secreted protein, acidic and rich in cysteine (SPARC) in GC. The function of hsa_circ_0017842/miR-1294/SPARC axis in GC cells was confirmed using gain- and loss-of-function assays. In addition, luciferase and RNA pulldown assays were performed to demonstrate the ceRNA mechanism of hsa_circ_0017842 involving miR-1294 and SPARC.

Results. The upregulation of hsa_circ_0017842 and SPARC, and downregulation of miR-1294 were observed in GC. Upregulating hsa_circ_0017842 in GC cells led to an increase in their proliferation, migration and invasion, and hsa_circ_0017842 knockdown showed the opposite effects on GC cells. Moreover, hsa_circ_0017842 was shown to be a sponge for miR-1294, thereby regulating SPARC expression. Due to the targeting relationship among hsa_circ_0017842, miR-1294 and SPARC, SPARC knockdown could relieve the effect of hsa_circ_0017842 overexpression on GC cells.

Conclusions. Overall, this study confirmed that hsa_circ_0017842 acted as a ceRNA to promote the malignancy of GC cells through regulating the miR-1294/SPARC axis. Our findings might help better elucidate the molecular mechanism of GC tumorigenesis, and as a result improve the overall survival of GC patients.

Key words: SPARC, ceRNA, gastric cancer, hsa_circ_0017842, miR-1294

Cite as
Wen X, Han W, Liu C. hsa_circ_0017842 acts as a competing endogenous RNA to enhance the malignancy of gastric cancer. *Adv Clin Exp Med*. 2023;32(7):803–812. doi:10.17219/acem/158484

DOI
10.17219/acem/158484

Background

Gastric cancer (GC), with high incidence and mortality, ranks among the top 5 malignant tumors and is the 3rd leading cause of cancer-related deaths worldwide.[1,2] According to the latest data from the World Health Organization (WHO) from 2020, the number of new GC cases in China was almost 480,000.[3] Although the incidence and mortality of GC decrease with the improvements in diagnosis and therapy, overall survival (OS) is poor in most countries due to the heterogeneity and complex regulatory mechanism of this disease.[4–6] Hence, exploring the molecular mechanism of GC tumorigenesis is an urgent need for improving the therapy of GC.

Circular RNAs (circRNAs) belong to the non-coding RNA family and exhibit a covalently closed-loop structure by direct back-splicing or exon skipping.[7,8] By means of high-throughput sequencing and bioinformatic analysis, circRNAs were confirmed to be abnormally expressed and participate in various diseases.[9–11] In GC, circRNAs have been shown to act as competing endogenous RNAs (ceRNAs) by regulating the expression of microRNAs (miRNAs) to release the target genes of miRNAs, thereby regulating GC progression.[12–14] The hsa_circ_0005556 acts as a ceRNA to sponge miR-4270-enhanced MMP19 expression, thereby accelerating GC progression.[15] The circRNA ITCH as a ceRNA could suppress the metastasis of GC cells by sponging miR-199a-5p/Klotho axis.[16] In the present study, we found the abnormal expression of hsa_circ_0017842 in GC samples using a circRNA expression microarray. To our knowledge, the function of hsa_circ_0017842 has not been reported. As a result of bioinformatic analysis, we predicted that hsa_circ_0017842 might sponge miR-1294. In GC, the inhibitory effect of miR-1294 on GC cells has been identified.[17–19] However, the circRNA as upstream of miR-1294 in GC is still unknown.

Secreted protein, acidic and rich in cysteine (SPARC), a matricellular glycoprotein, is expressed in embryonic tissues, bone and endothelial cells, and has been shown to play a key role in the development and differentiation of chondrocytes and megakaryocytes.[20,21] Clinically, *SPARC* was found to be overexpressed in GC tissues, and its overexpression was correlated with the poor survival rate of GC patients with tumor-node-metastasis (TNM) stages I, II and III.[22] In in vitro studies, knocking down SPARC reduced the number of invasive GC cells, suggesting its promotive function in GC development.[23] Bioinformatic analysis in our study predicted that *SPARC* was a target gene of miR-1294. Furthermore, the interaction between miR-1294 and SPARC has not been explored in any diseases.

Objectives

By means of a literature review and bioinformatic analysis, we aimed to investigate whether hsa_circ_0017842 acts as a crucial circRNA to regulate GC progression by targeting the miR-1294/SPARC pathway. Our findings could contribute to elucidating the molecular mechanism of GC tumorigenesis to improve the overall survival of GC patients.

Materials and methods

Bioinformatic analysis

GSE93541 from a public database (GEO DataSets; https://www.ncbi.nlm.nih.gov/gds) was used to identify the expression of hsa_circ_0017842 in GC samples and normal samples from the same patients. Then, starBase (https://starbase.sysu.edu.cn/panCancer.php) and circInteractome database (https://starbase.sysu.edu.cn/panCancer.php) were applied to predict the downstream miRNAs of hsa_circ_0017842, whereas TargetScan database (https://starbase.sysu.edu.cn/panCancer.php) was used to predict the downstream mRNAs of the predicted miRNAs. Besides, we also used 2 gene expression microarrays (GSE103236 and GSE79973) from GEO DataSets to confirm the upregulated genes in GC with adjusted $p < 0.05$ and $\log_2 FC > 1$. STRING tool (https://cn.string-db.org/) was used to construct protein-protein interaction (PPI) networks for the screened genes.

Clinical samples and cell lines

The GC samples and corresponding adjacent non-tumor samples were collected from 34 patients who were diagnosed with GC in the Third People's Hospital of Hubei Province (Wuhan, China) between January 2021 and January 2022. Our study was approved by the Ethics Committee of the Third People's Hospital of Hubei Province (2021 Ethic Audit Section No. 16) and adheres to the ethical standards of the Declaration of Helsinki. Every patient enrolled in this study gave written informed consent.

Table 1 displays the clinical characteristics of 34 GC patients. All cell lines were purchased from Procell (Wuhan, China), including 2 GC cell lines (AGS, cat. No. CL-0022; MKN-7 and cat No. CL-0574) and human gastric mucosa cell line GES-1 (cat. No. CL-0563). The AGS cells were kept in Ham's F-12 medium (cat No. PM150810; Procell) at 37°C and 5% CO_2, whereas GES-1 and MKN-7 cells were kept in RPMI-1640 medium (cat. No. PM150110; Procell) at 37°C and 5% CO_2. All media were supplemented with 10% fetal bovine serum (FBS; cat. No. 164210-50; Procell) and 1% penicillin/streptomycin (cat. No. PB180120; Procell).

Table 1. Clinical characteristics of the gastric cancer patients

Characteristics		Numbers of cases (%)
Age [years]	≥60 <60	19 (55.9) 15 (44.1)
Gender	male female	22 (64.7) 12 (35.3)
Tumor size	<3 cm ≥3cm	14 (41.2) 20 (58.8)
TNM stage	I + II III + IV	9 (26.5) 25 (73.5)
Grade	well moderately poor	5 (14.7) 20 (58.8) 9 (26.5)

TNM – tumor-node-metastasis.

qPCR and RNase R treatment

TRIzol Total RNA isolation kit (cat. No. KGA1201; KeyGen Biotech, Nanjing, China) was used for RNA extraction from tissues and cells. Then, cDNA synthesis and quantitative real-time polymerase chain reaction (qPCR) were carried out using a PrimeScript Reverse Transcription Kit (Takara, Shiga, Japan) and SYBR Green Master Mix Kit (Takara), respectively. The $2^{-\Delta\Delta Ct}$ method was applied for identifying the relative expression of circRNA, miRNA and mRNA using GAPDH or U6 as an endogenous control. Table 2 includes all the primer sequences used in this study.

For RNase R treatment, 2 μg of isolated RNA from GC cells were treated with or without 3 U/mg RNase R (Sigma-Aldrich, St. Louis, USA). After incubation for 60 min at 37°C, the expression of hsa_circ_0017842 and its linear gene *FAM188A* was measured with qPCR to demonstrate the stability of hsa_circ_0017842.

Table 2. Primer sequences in this study

Gene		Primer sequence
hsa_circ_0017842	forward	5′-TGATCCTAGTTGATGGCCTAA-3′
	reverse	5′-GAGAGCCACTTGCAGAGACC-3′
hsa-miR-1270	forward	5′-CTGGAGATATGGAAGAGCTGTGT-3′
	reverse	5′-TGCAAAGAGCCACATAGAAGAT-3′
hsa-miR-620	forward	5′-GCCGAGATGGAGATAGATAT-3′
	reverse	5′-CTCAACTGGTGTCGTGGA-3
hsa-miR-1294	forward	5′-CTTAGTTGCGTTACACCCTTTCTTG–3′
	reverse	5′-CTGTCACCTTCACCGTTCCAGTTT–3′
hsa-miR-1286	forward	5′-GCCGAGTGCAGGACCAAGATG–3′
	reverse	5′-CTCAACTGGTGTCGTGGA–3′
SPARC	forward	5′-CGAAGAGGAGGTGGTGGCGGAAA–3′
	reverse	5′-GGTTGTTGTCCTCATCCCTCTCATAC–3′
GAPDH	forward	5′-CTCTCTGCTCCTCCTGTTCGACAG-3′
	reverse	5′-AGGGGTCTTACTCCTTGGAGGCCA-3′
U6	forward	5′-CTCGCTTCGGCAGCACA-3′
	reverse	5′-AACGCTTCACGAATTTGCGT-3′

Cell transfection

All vectors used for cell transfection were purchased from Ke Lei Biological Technology Co., Ltd. (Shanghai, China). The pcDNA3.1-circ vector was used to construct hsa_circ_0017842 expression vectors (circ-OE), and the empty vector was used as a negative control (NC). The siRNAs targeting hsa_circ_0017842 (si-circ) and *SPARC* (si-SPARC) were used to knock down hsa_circ_0017842 and SPARC, respectively, with si-NC as NC. The miR-1294 mimic was designed to overexpress miR-1294 and mimic-NC was used as NC. For cell transfections, the mentioned vectors were applied to the GC cells at 50 nM concentration using Lipofectamine 3000 (Invitrogen, Carlsbad, USA). The qPCR was carried out to identify the transfection efficiency of vectors 48 h after transfection.

EdU assay

EdU-647 cell proliferation kit (Beyotime Biotechnology, Beijing, China) was used to assess cell proliferation. After transfection, 1×10^4 GC cells were seeded into a 96-well plate for incubation overnight. After incubation, 10 μM EdU was applied to cells for 2 h at 37°C. Then, the cells were fixed with 4% paraformaldehyde, treated with 0.1% Triton X-100, rinsed with phosphate-buffered saline (PBS), and incubated with 100 μL click reaction cocktail. Next, the cells were incubated in 5 μg/mL Hoechst 33342 to stain cell nuclei. Finally, the cells were observed and imaged using a fluorescence microscope (model TE2000; Nikon Corp., Tokyo, Japan).

Transwell assay

Transwell assays were performed to assess the change in cell migration and invasion. In cell migration detection, 1×10^4 transfected GC cells suspended in 200 μL of serum-free medium were added into the upper chamber; at the same time, 500 μL of medium with 10% FBS was added into the bottom chamber. After 48 h, the cells that remained on the lower surface were fixed with methanol, stained with crystal violet and observed under an inverted micoscope (model TS2; Nikon Corp.). In cell invasion detection, the membrane in the upper chamber was coated with Matrigel (BD Biosciences, Franklin Lakes, USA) before adding the cells. The following procedure was the same as cell migration.

RNA pulldown assay

A biotinylated RNA pulldown assay was used to identify the interaction between circRNA and miRNA, as described in a previous study.[24] Briefly, 1×10^7 GC cells were collected, lysed, and incubated with hsa_circ_0017842 probe-coated beads at 4°C overnight. After washing, the RNA was isolated to perform qPCR.

Luciferase assay

Wild-type hsa_circ_0017842 (WT-circ) or SPARC (SPARC-WT) containing binding sites for miR-1294 were constructed by Beijing Qualityard Biotechnology Co., Ltd. (Beijing, China) using a pGL3 vector (Promega, Madison, USA). Mutant hsa_circ_0017842 (MUT-circ) or SPARC (SPARC-MUT) without binding sites for miR-1294 were also constructed by Beijing Qualityard Biotechnology Co., Ltd. using a pGL3 vector. The aforementioned vectors were co-transfected into GC cells with miR-1294 mimic or mimic-NC. Luciferase activity was detected 48 h after transfection with the aid of a dual-luciferase report analysis system (Promega).

Western blotting

Protein concentrations, isolated using Radioimmunoprecipitation Assay (RIPA) Lysis Buffer (cat. No. KGP702; KeyGen Biotech), were quantified with BCA Protein Assay Kit (Tiangen Biotech, Beijing, China). Protein samples were separated using 12% sodium dodecyl-sulfate polyacrylamide gel electrophoresis (SDS-PAGE) gel, then transferred to polyvinylidene difluoride (PVDF) membranes and blocked with 5% skimmed milk for 3 h at 22°C. The membranes were incubated overnight at 4°C with primary antibodies, including anti-SPARC (1:1000; cat. No. ab207743; Abcam, Cambridge, USA) and anti-GAPDH (1:1000; cat. No. ab9485; Abcam). Next, the membranes were probed with fluorescent rabbit secondary antibodies (cat. No. 18-4517-32; Rockland Immunochemicals, Rockland, USA) at 22°C for 2 h. Finally, the protein blots were visualized using Odyssey 3.2 (LI-COR Biosciences, Lincoln, USA).

Statistical analyses

Independent experiments were performed in triplicate. The data were analyzed using GraphPad Prism v. 8.0 (GraphPad Software, San Diego, USA) and expressed as the mean ± standard deviation (M ±SD). Each independent experiment included at least 3 samples. Shapiro–Wilk test was used to confirm the normal distribution of all data, and F test/Brown–Forsythe test was used to confirm the homogeneity of variances. Student's t-test was applied for statistical differences between the 2 groups, whereas Kruskal–Wallis test with Dunn's post hoc test or Mann–Whitney U test was applied for statistical differences if the number of samples was ≤9. A value of $p < 0.05$ denotes statistical significance.

Results

The upregulation of hsa_circ_0017842 in GC

According to a circRNA expression microarray GSE93541, hsa_circ_0017842 was overexpressed in GC samples compared to normal non-tumor samples (Fig. 1A). In our collected clinical samples, hsa_circ_0017842 was

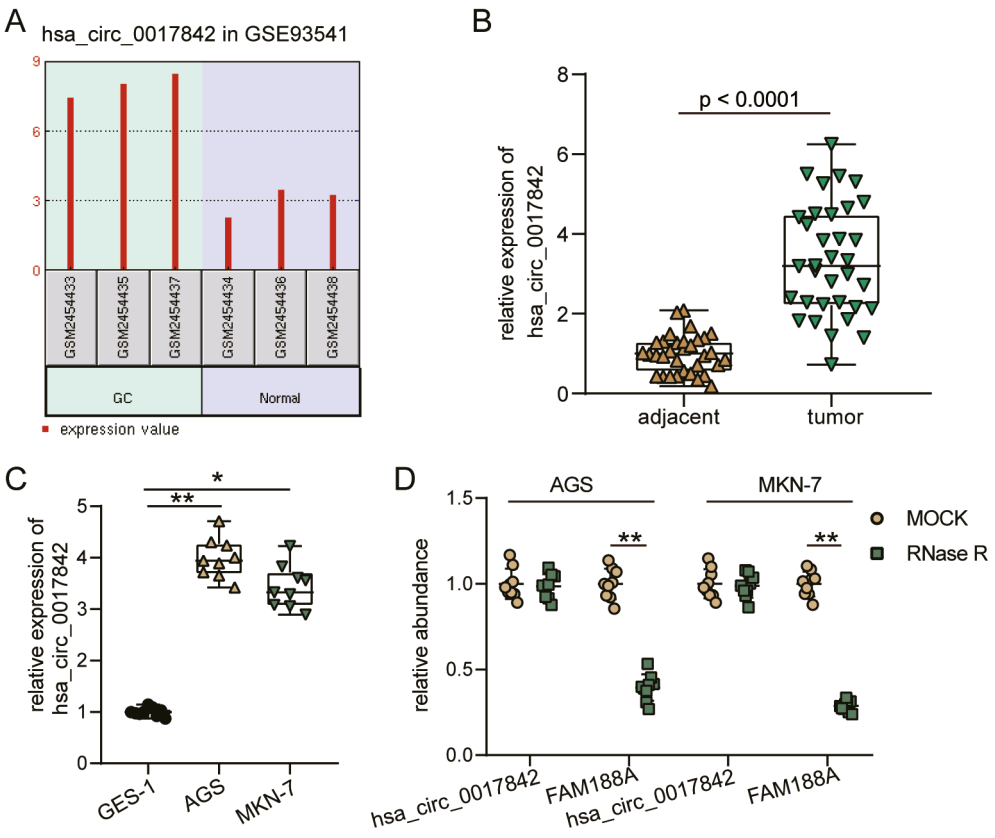

Fig. 1. The upregulation of hsa_circ_0017842 in gastric cancer (GC). A. A circular RNA (circRNA) expression microarray GSE93541 identified the upregulation of hsa_circ_0017842 in GC samples; B. hsa_circ_0017842 overexpression in GC tissues was detected using quantitative real-time polymerase chain reaction (qPCR) (paired Student's t-test, n = 34); C. hsa_circ_0017842 overexpression in GC cells (AGS and MKN-7) was detected using qPCR (*$p < 0.05$, **$p < 0.01$; Kruskal–Wallis test; n = 9); D. RNase R treatment confirmed the stable structure of hsa_circ_0017842 (**$p < 0.01$; Mann–Whitney U test; n = 9). All experiments were performed in triplicate

also upregulated in GC samples compared to adjacent normal samples (Fig. 1B). In GC cells (AGS and MKN-7), hsa_circ_0017842 expression was significantly elevated (Fig. 1C). RNase R treatment did not produce any change in hsa_circ_0017842 expression, suggesting that the structure of hsa_circ_0017842 was stable (Fig. 1D). To summarize, hsa_circ_0017842 exhibited a stable structure and was overexpressed in GC.

The positive effect of hsa_circ_0017842 on GC cells

To explore the effect of hsa_circ_0017842 on GC cells, we transfected circ-OE vectors and si-circ to overexpress and knock down hsa_circ_0017842 in GC cells, respectively. Figure 2A displays the increase of hsa_circ_0017842 expression by more than 6-fold in GC cells after transfection with circ-OE vectors, whereas its expression decreased by more than 70% in GC cells after transfection with si-circ. The EdU assays revealed that circ-OE elevated EDU positive rate, but si-circ caused a decline of EDU positive rate, suggesting the positive effect of hsa_circ_0017842 on cell proliferation (Fig. 2B). The transwell assay identified an increase in the number of migration cells and invasion cells after the GC cells were transfected with circ-OE, but showed a decrease after the GC cells were transfected with si-circ (Fig. 2C,D). All data suggested that hsa_circ_0017842 contributed to the proliferation, migration and invasion of GC cells.

hsa_circ_0017842 as a ceRNA to target miR-1294

To identify the miRNAs that bind to hsa_circ_0017842, 2 online databases (starBase and TargetScan) were used and 4 miRNAs were identified (miR-620, miR-1270, miR-1294, and miR-1286; Fig. 3A). RNA pulldown assays confirmed that only miR-1294 could be pulled down from GC cell samples with the hsa_circ_0017842 probe (Fig. 3B). Hence, we chose miR-1294 for further investigation. The binding

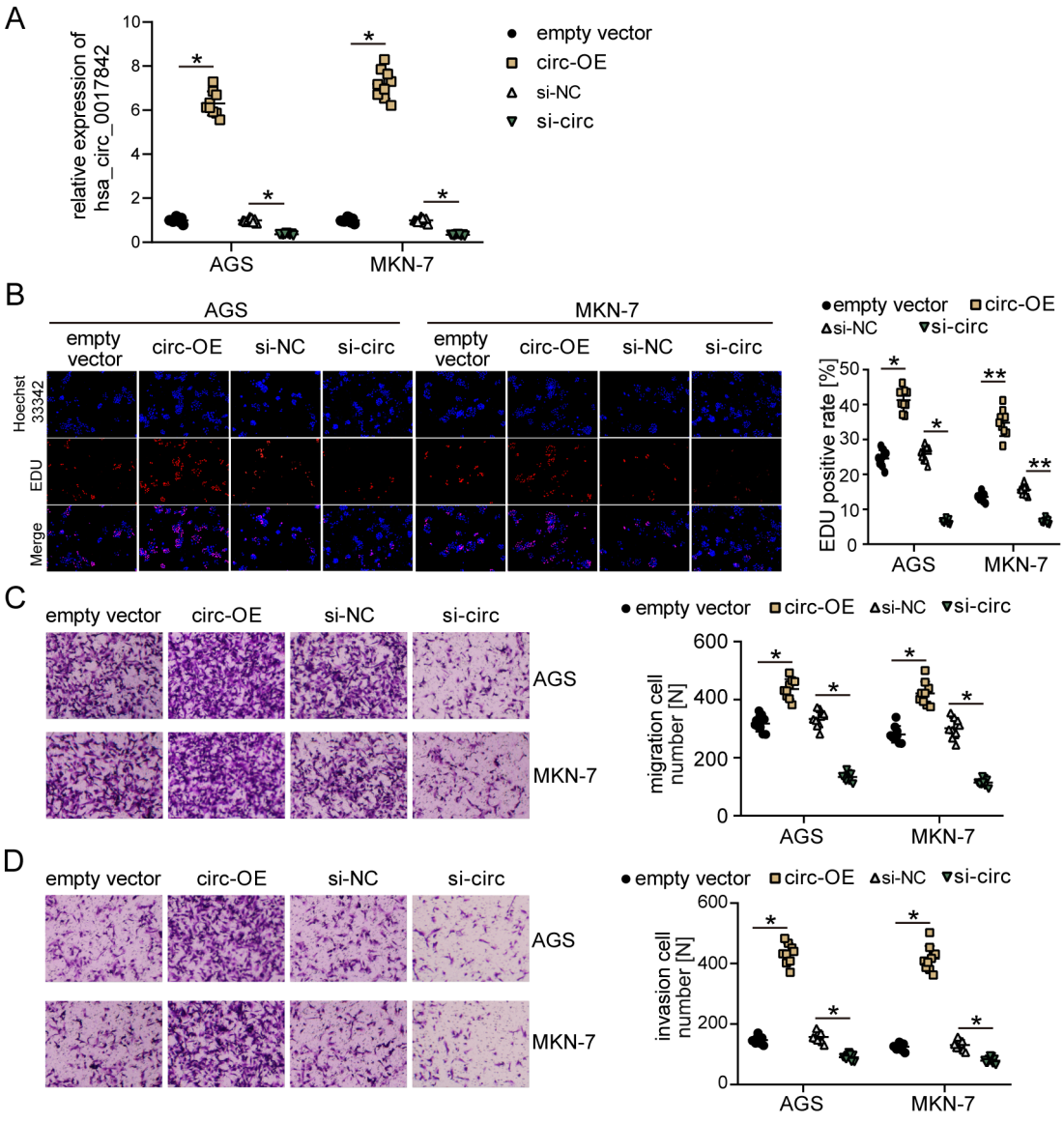

Fig. 2. The positive effect of hsa_circ_0017842 on gastric cancer (GC) cells. A. High transfection efficiency of the hsa_circ_0017842 overexpression vector (circ-OE) and siRNA of hsa_circ_0017842 (si-circ) was confirmed using quantitative real-time polymerase chain reaction (qPCR); B. The positive effect of hsa_circ_0017842 on cell proliferation in GC cells was detected using EdU assay; C,D. Transwell assay showed that hsa_circ_0017842 promoted cell migration (C) and cell invasion (D)

*p < 0.05, **p < 0.01; Kruskal–Wallis test; n = 9. All experiments were performed in triplicate.

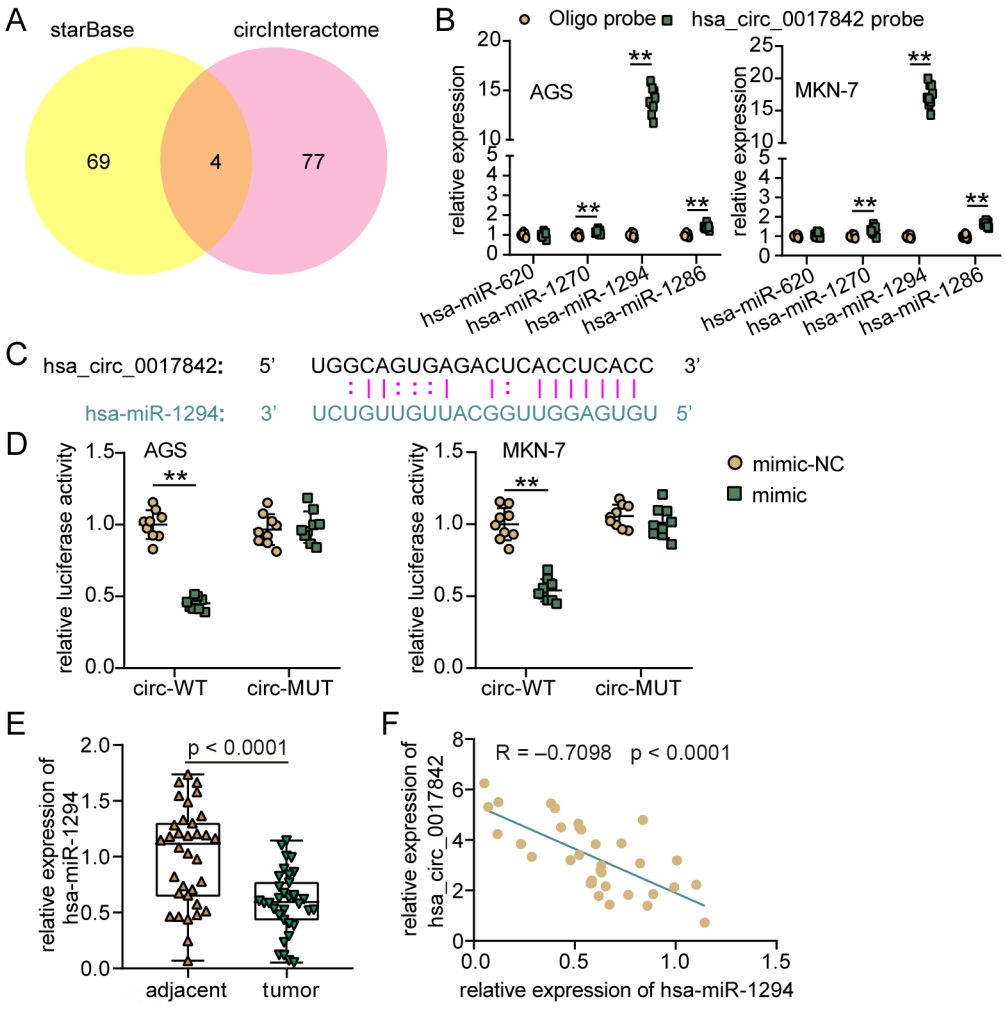

Fig. 3. hsa_circ_0017842 as a ceRNA to target miR-1294. A. starBase and circInteractome predicted miRNAs binding to hsa_circ_0017842; B. The interaction between hsa_circ_0017842 and miR-1294 was confirmed using RNA pulldown assay (**p < 0.01; Mann–Whitney U test; n = 9); C. The binding sites between hsa_circ_0017842 and miR-1294; D. The binding sites between hsa_circ_0017842 and miR-1294 were confirmed with luciferase assay (**p < 0.01; Kruskal–Wallis test; n = 9); E. The downregulation of miR-1294 in GC tissues was detected using quantitative real-time polymerase chain reaction (qPCR) (paired Student's t-test; n = 34); F. The negative correlation between hsa_circ_0017842 and miR-1294 was analyzed with Pearson's correlation analysis. All experiments were performed in triplicate

sites between hsa_circ_0017842 and miR-1294 are shown in Fig. 3C. According to the binding sites, the circ-WT with binding sites and circ-MUT without binding sites were designed to perform a luciferase assay. The miR-1294 mimic reduced the luciferase activity in the circ-WT group but not in the circ-MUT group, suggesting that miR-1294 could bind to hsa_circ_0017842 (Fig. 3D). Compared with adjacent normal tissues, miR-1294 expression was significantly downregulated in GC tissues ($p < 0.0001$, Fig. 3E). After Pearson's correlation analysis, hsa_circ_0017842 expression and miR-1294 expression in GC samples displayed a negative correlation (Fig. 3F). In conclusion, miR-1294 is downregulated in GC samples and could be sponged by hsa_circ_0017842.

SPARC as a target gene of miR-1294

To predict the target genes of miR-1294, TargetScan database was used. At the same time, GSE103236 and GSE79973 mRNA microarrays were performed using GC samples and adjacent normal samples to identify the upregulated genes. Finally, 21 genes were screened from TargetScan, GSE103236 and GSE79973 (Fig. 4A). The PPI network of the 21 screened genes was constructed using the STRING tool (Fig. 4B) because *SPARC* connected the most genes in network. Therefore, *SPARC* was selected as the key gene to be explored. Figure 4C displays the binding sites between *SPARC* and miR-1294. After performing a luciferase assay, it was found that luciferase activity was reduced in the SPARC-WT group only when GC cells were transfected with miR-1294 mimic (Fig. 4D). The *SPARC* expression was upregulated almost 3-fold in GC samples (Fig. 4E), and its expression was negatively related to miR-1294 expression in GC samples (Fig. 4F). These results confirmed that *SPARC* was overexpressed in GC samples and is a target of miR-1294.

Silencing *SPARC* reversed the positive role of hsa_circ_0017842 overexpression in GC cells

To identify whether the effect of hsa_circ_0017842 on GC cells could be regulated by SPARC, we transfected si-SPARC and circ-OE into GC cells to perform the following experiments. Western blotting showed that circ-OE induced a >1.5-fold increase in the expression of SPARC protein, whereas si-SPARC decreased the expression of SPARC protein by approx. 50% (Fig. 5A). However,

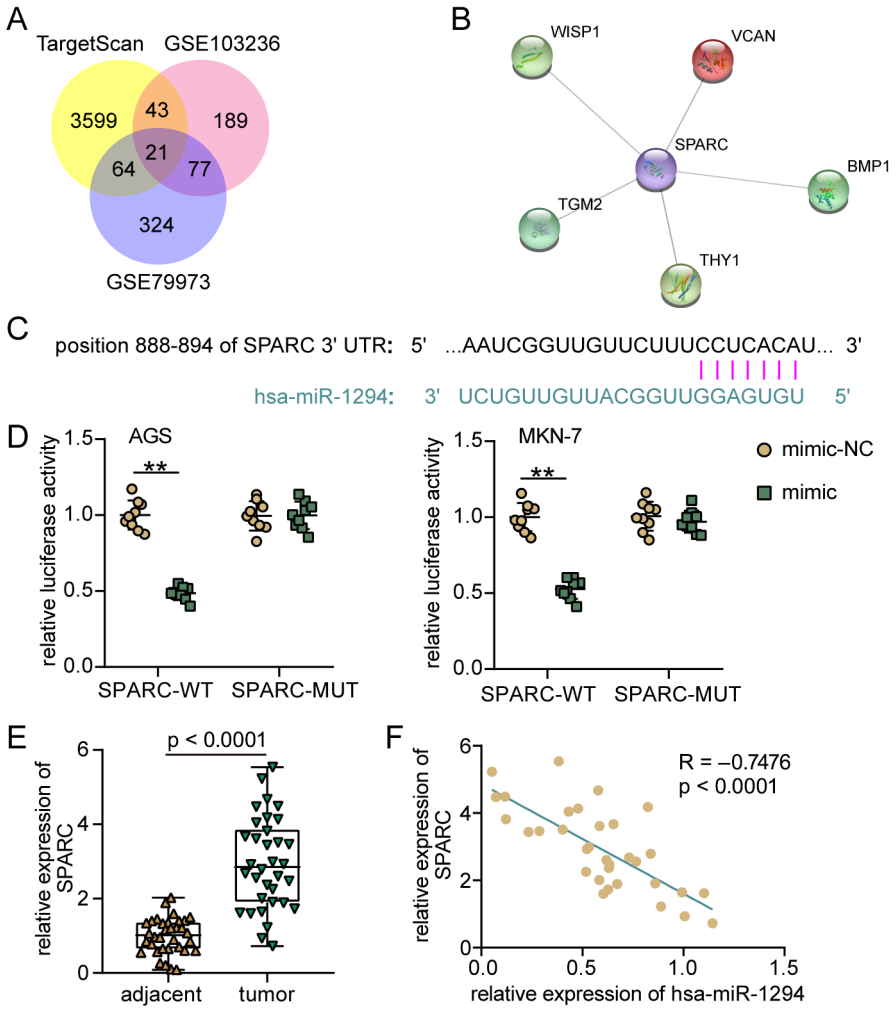

Fig. 4. *SPARC* as a target gene of miR-1294. A. 21 genes were screened from TargetScan, GSE103236, and GSE79973. TargetScan was used to predict the target genes of miR-1294. GSE103236 and GSE79973 are 2 mRNA microarrays used to screen for upregulated genes that satisfy the criteria: adjusted $p < 0.05$ and $\log_2FC>1$; B. SPARC was the center of the PPI network constructed using STRING tool; C. The binding sites between *SPARC* and miR-1294; D. The binding sites between SPARC and miR-1294 were confirmed with luciferase assay (**$p < 0.01$; Kruskal–Wallis test; $n = 9$); E. *SPARC* overexpression in GC tissues was detected using quantitative real-time polymerase chain reaction (qPCR) (paired Student's t-test; $n = 34$); F. Negative correlation between *SPARC* and miR-1294 was analyzed using Pearson's correlation analysis. All experiments were performed in triplicate

co-transfection of si-SPARC and circ-OE did not change the expression of SPARC protein compared with empty vector or si-NC groups (Fig. 5A). The results of EdU assay suggested that si-SPARC suppressed cell proliferation and reversed the circ-OE-induced increase in cell proliferation (Fig. 5B). Likewise, si-SPARC resulted in less cell migration, and it reversed the enhancement of cell migration caused by circ-OE (Fig. 5C). A consistent result was reproduced in cell invasion, showing that silencing *SPARC* reduced the number of invasive cells and attenuated the circ-OE-mediated enhancement of cell invasion (Fig. 5D). Taken together, we showed that the positive role of hsa_circ_0017842 overexpression in GC cells was reversed through silencing *SPARC*.

Discussion

The circRNAs are considered to play crucial roles in GC progression through a ceRNA mechanism.[12,25,26] In the present study, we found that hsa_circ_0017842 was overexpressed in GC and enhanced the proliferation, migration and invasion of GC cells. Moreover, hsa_circ_0017842 acted as a ceRNA to regulate the miR-1294/SPARC axis in GC cells. Due to the interactions between hsa_circ_0017842, miR-1294 and *SPARC*, *SPARC* knockdown could reverse the positive effect of hsa_circ_0017842 on GC progression.

The abnormal expression of circRNAs was detected in GC, and different circRNAs were found to play different roles in GC.[27,28] For instance, high expression of circ-SHKBP1 was related to advanced TNM stage and poor prognosis in GC, and its overexpression promoted cell metastasis and angiogenesis of GC cells.[29] Another circRNA located in the nucleus, circ-HuR, could attenuate tumor growth and metastasis of GC cells in vivo.[30] Here, we used a circRNA microarray of GC from GEO DataSets and qPCR to identify the upregulation of hsa_circ_0017842 in GC samples. By a series of gain-or-loss experiments, hsa_circ_0017842 was confirmed to be an oncogenic circRNA in GC which promotes proliferation, migration and invasion of GC cells.

In recent years, increasing evidence has demonstrated that circRNAs acting as ceRNAs participate in GC progression by sponging miRNAs to regulate target genes of miRNAs.[31–33] Zhang et al. reported that circ_HN1, miR-628-5p and Ecto-5'-nucleotidase could construct a ceRNA network to regulate GC development.[33] The circ-ITCH as a ceRNA regulated the miR-199a-5p/Klotho axis,

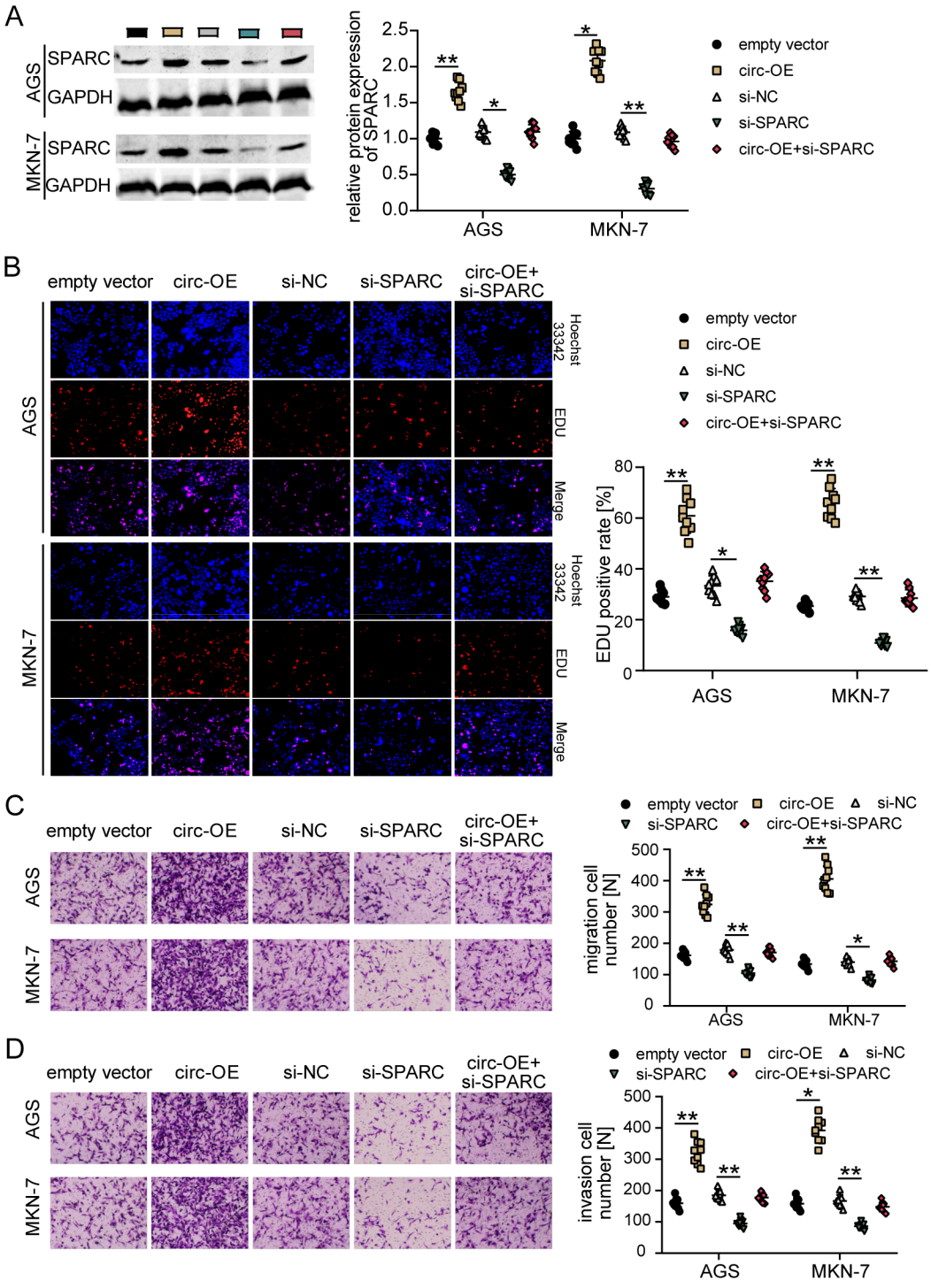

Fig. 5. Silencing *SPARC* diminished the positive effect of hsa_circ_0017842 overexpression on GC cells. A. Western blotting detected the expression of SPARC in transfected GC cells; B. The positive effect of hsa_circ_0017842 overexpression on cell proliferation was reversed by silencing *SPARC*; C,D. Silencing *SPARC* recovered the effect of hsa_circ_0017842 overexpression on cell migration (C) and cell invasion (D)

*p < 0.05, **p < 0.01; Kruskal–Wallis test; n = 9. All experiments were performed in triplicate.

thereby inhibiting metastasis of GC cells.[16] However, no study identified a ceRNA network of hsa_circ_0017842. Innovatively, we used bioinformatic analysis and in vitro experiments to demonstrate that hsa_circ_0017842 could be a ceRNA that sponges miR-1294, thereby enhancing *SPARC* expression in GC cells. This means that we constructed a novel ceRNA network on hsa_circ_0017842 to participate in GC progression, which enriched the regulatory network of GC.

The function of SPARC in GC has been explored in several studies. Clinically, *SPARC* was found to be upregulated in GC tissues, and its overexpression predicted a poor survival rate of GC.[22] In vitro, *SPARC* knockdown in GC cells reduced cell invasion and enhanced cell apoptosis, suggesting the oncogenic function of *SPARC* in GC cells.[23] Consistent with previous studies, we also observed the upregulation of *SPARC* in GC tissues and cells, while silencing *SPARC* suppressed the proliferation, migration and invasion of GC cells. However, whether circRNA could regulate *SPARC* by ceRNA network in GC has not been confirmed yet. In this study, we have revealed for the first time that hsa_circ_0017842 is upstream of *SPARC*

by sponging miR-1294 to upregulate *SPARC* expression, thereby eliminating the inhibitory effect of *SPARC* knockdown on GC cells.

Limitations

Our study revealed the function and mechanism of hsa_circ_0017842 in GC development. However, whether hsa_circ_0017842 can affect the malignancy of GC cells in vivo has not been investigated. Lymph node metastasis has been found to be associated with tumor development[34,35]; therefore, we will explore the relationship between hsa_circ_0017842 and lymph node metastasis in GC samples in the future. Furthermore, the role of hsa_circ_0017842 in GC in a clinical setting, such as GC prognosis, chemotherapy resistance, as a drug target, etc., is still not explored. In our further research, we will focus on these areas.

Conclusions

Our study demonstrated that hsa_circ_0017842 acted as a competing endogenous RNA to enhance the malignancy of GC by sponging miR-1294 to upregulate *SPARC*. The function of hsa_circ_0017842 in GC is identified, which may provide a novel target for GC therapy in the years to come.

ORCID iDs

Xigang Wen https://orcid.org/0000-0002-8509-9323
Wenling Han https://orcid.org/0000-0003-4240-6319
Chao Liu https://orcid.org/0000-0001-9355-3146

References

1. Sung H, Ferlay J, Siegel RL, et al. Global cancer statistics 2020: GLOBOCAN estimates of incidence and mortality worldwide for 36 cancers in 185 countries. *CA A Cancer J Clin*. 2021;71(3):209–249. doi:10.3322/caac.21660
2. Etemadi A, Safiri S, Sepanlou SG, et al. The global, regional, and national burden of stomach cancer in 195 countries, 1990–2017: A systematic analysis for the Global Burden of Disease study 2017. *Lancet Gastroenterol Hepatol*. 2020;5(1):42–54. doi:10.1016/S2468-1253(19)30328-0
3. Li K, Zhang A, Li X, Zhang H, Zhao L. Advances in clinical immunotherapy for gastric cancer. *Biochim Biophys Acta Rev Cancer*. 2021;1876(2):188615. doi:10.1016/j.bbcan.2021.188615
4. Allemani C, Weir HK, Carreira H, et al. Global surveillance of cancer survival 1995–2009: Analysis of individual data for 25,676,887 patients from 279 population-based registries in 67 countries (CONCORD-2). *Lancet*. 2015;385(9972):977–1010. doi:10.1016/S0140-6736(14)62038-9
5. Tan P, Yeoh KG. Genetics and molecular pathogenesis of gastric adenocarcinoma. *Gastroenterology*. 2015;149(5):1153–1162.e3. doi:10.1053/j.gastro.2015.05.059
6. Nakamura J. Methylation-mediated gene silencing as biomarkers of gastric cancer: A review. *World J Gastroenterol*. 2014;20(34):11991–12006. doi:10.3748/wjg.v20.i34.11991
7. Qu S, Yang X, Li X, et al. Circular RNA: A new star of noncoding RNAs. *Cancer Lett*. 2015;365(2):141–148. doi:10.1016/j.canlet.2015.06.003
8. Memczak S, Jens M, Elefsinioti A, et al. Circular RNAs are a large class of animal RNAs with regulatory potency. *Nature*. 2013;495(7441):333–338. doi:10.1038/nature11928
9. Li J, Sun D, Pu W, Wang J, Peng Y. Circular RNAs in cancer: Biogenesis, function, and clinical significance. *Trends Cancer*. 2020;6(4):319–336. doi:10.1016/j.trecan.2020.01.012
10. Jia N, Li J. Role of circular RNAs in preeclampsia. *Dis Markers*. 2019;2019:7237495. doi:10.1155/2019/7237495
11. Gu W, Sun Y, Zheng X, et al. Identification of gastric cancer-related circular RNA through microarray analysis and bioinformatics analysis. *Biomed Res Int*. 2018;2018:2381680. doi:10.1155/2018/2381680
12. Guan YJ, Ma JY, Song W. Identification of circRNA–miRNA–mRNA regulatory network in gastric cancer by analysis of microarray data. *Cancer Cell Int*. 2019;19(1):183. doi:10.1186/s12935-019-0905-z
13. Luo Z, Rong Z, Zhang J, et al. Circular RNA circCCDC9 acts as a miR-6792-3p sponge to suppress the progression of gastric cancer through regulating CAV1 expression. *Mol Cancer*. 2020;19(1):86. doi:10.1186/s12943-020-01203-8
14. Guo LL. Competing endogenous RNA networks and gastric cancer. *World J Gastroenterol*. 2015;21(41):11680–11687. doi:10.3748/wjg.v21.i41.11680
15. Shen D, Zhao H, Zeng P, et al. Circular RNA hsa_circ_0005556 accelerates gastric cancer progression by sponging miR-4270 to increase MMP19 expression. *J Gastric Cancer*. 2020;20(3):300–312. doi:10.5230/jgc.2020.20.e28
16. Wang Y, Wang H, Zheng R, et al. Circular RNA ITCH suppresses metastasis of gastric cancer via regulating miR-199a-5p/Klotho axis. *Cell Cycle*. 2021;20(5–6):522–536. doi:10.1080/15384101.2021.1878327
17. Wang Y, Liu G, Sun S, Qin J. miR-1294 alleviates epithelial–mesenchymal transition by repressing FOXK1 in gastric cancer. *Genes Genom*. 2020;42(2):217–224. doi:10.1007/s13258-019-00899-3
18. Wu D, Li H, Wang J, et al. LncRNA NEAT1 promotes gastric cancer progression via miR-1294/AKT1 axis. *Open Med*. 2020;15(1):1028–1038. doi:10.1515/med-2020-0218
19. Shi YX, Ye BL, Hu BR, Ruan XJ. Expression of miR-1294 is downregulated and predicts a poor prognosis in gastric cancer. *Eur Rev Med Pharmacol Sci*. 2018;22(17):5525–5530. doi:10.26355/eurrev_201809_15813
20. Podhajcer OL, Benedetti LG, Girotti MR, Prada F, Salvatierra E, Llera AS. The role of the matricellular protein SPARC in the dynamic interaction between the tumor and the host. *Cancer Metastasis Rev*. 2008;27(4):691–705. doi:10.1007/s10555-008-9146-7
21. Yan Q, Sage EH. SPARC, a matricellular glycoprotein with important biological functions. *J Histochem Cytochem*. 1999;47(12):1495–1505. doi:10.1177/002215549904701201
22. Zhao ZS, Wang YY, Chu YQ, Ye ZY, Tao HQ. SPARC is associated with gastric cancer progression and poor survival of patients. *Clin Cancer Res*. 2010;16(1):260–268. doi:10.1158/1078-0432.CCR-09-1247
23. Yin J, Chen G, Liu Y, et al. Downregulation of SPARC expression decreases gastric cancer cellular invasion and survival. *J Exp Clin Cancer Res*. 2010;29(1):59. doi:10.1186/1756-9966-29-59
24. Wang K, Long B, Liu F, et al. A circular RNA protects the heart from pathological hypertrophy and heart failure by targeting miR-223. *Eur Heart J*. 2016;37(33):2602–2611. doi:10.1093/eurheartj/ehv713
25. Zhang X, Wang S, Wang H, et al. Circular RNA circNRIP1 acts as a microRNA-149-5p sponge to promote gastric cancer progression via the AKT1/mTOR pathway. *Mol Cancer*. 2019;18(1):20. doi:10.1186/s12943-018-0935-5
26. Peng L, Sang H, Wei S, et al. circCUL2 regulates gastric cancer malignant transformation and cisplatin resistance by modulating autophagy activation via miR-142-3p/ROCK2. *Mol Cancer*. 2020;19(1):156. doi:10.1186/s12943-020-01270-x
27. Ghafouri-Fard S, Honarmand Tamizkar K, Jamali E, Taheri M, Ayatollahi SA. Contribution of circRNAs in gastric cancer. *Pathol Res Pract*. 2021;227:153640. doi:10.1016/j.prp.2021.153640
28. Fang X, Wen J, Sun M, Yuan Y, Xu Q. CircRNAs and its relationship with gastric cancer. *J Cancer*. 2019;10(24):6105–6113. doi:10.7150/jca.32927
29. Xie M, Yu T, Jing X, et al. Exosomal circSHKBP1 promotes gastric cancer progression via regulating the miR-582-3p/HUR/VEGF axis and suppressing HSP90 degradation. *Mol Cancer*. 2020;19(1):112. doi:10.1186/s12943-020-01208-3
30. Yang F, Hu A, Li D, et al. Circ-HuR suppresses HuR expression and gastric cancer progression by inhibiting CNBP transactivation. *Mol Cancer*. 2019;18(1):158. doi:10.1186/s12943-019-1094-z

31. Li X, Li Z, Liu P, et al. Novel circRNAs in hub ceRNA axis regulate gastric cancer prognosis and microenvironment. *Front Med (Lausanne)*. 2021;8:771206. doi:10.3389/fmed.2021.771206
32. Xia T, Pan Z, Zhang J. CircPDZD8 promotes gastric cancer progression by regulating CHD9 via sponging miR-197-5p. *Aging (Albany NY)*. 2020;12(19):19352–19364. doi:10.18632/aging.103805
33. Zhang J, Wang F, Zhang H, Cao M. A novel circular RNA circ_HN1/miR-628-5p/Ecto-5′-nucleotidase competing endogenous RNA network regulates gastric cancer development. *Bioengineered*. 2021;12(2): 9739–9752. doi:10.1080/21655979.2021.1989259
34. Isik A, Soran A, Grasi A, Barry N, Sezgin E. Lymphedema after sentinel lymph node biopsy: Who is at risk? *Lymph Res Biol*. 2022;20(2): 160–163. doi:10.1089/lrb.2020.0093
35. Işık A, Fırat D, Peker K, İnal A, Yılmaz İ, Çelebi F. Breast skin necrosis after methylene blue dye injection: Breast image. *Sakarya Med J*. 2018;8(1):153–156. doi:10.31832/smj.376329